

Supplemental information

Integrating IL-12 mRNA nanotechnology with SBRT

eliminates T cell exhaustion in preclinical

models of pancreatic cancer

Angela L. Hughson, Gary Hannon, Noah A. Salama, Tara G. Vrooman, Caroline A. Stockwell, Bradley N. Mills, Jesse Garrett-Larsen, Haoming Qiu, Roula Katerji, Lauren Benoodt, Carl J. Johnston, Joseph D. Murphy, Emma Kruger, Jian Ye, Nicholas W. Gavras, David C. Keeley, Shuyang S. Qin, Maggie L. Lesch, Jason B. Muhitch, Tanzy M.T. Love, Laura M. Calvi, Edith M. Lord, Nadia Luheshi, Jim Elyes, David C. Linehan, and Scott A. Gerber

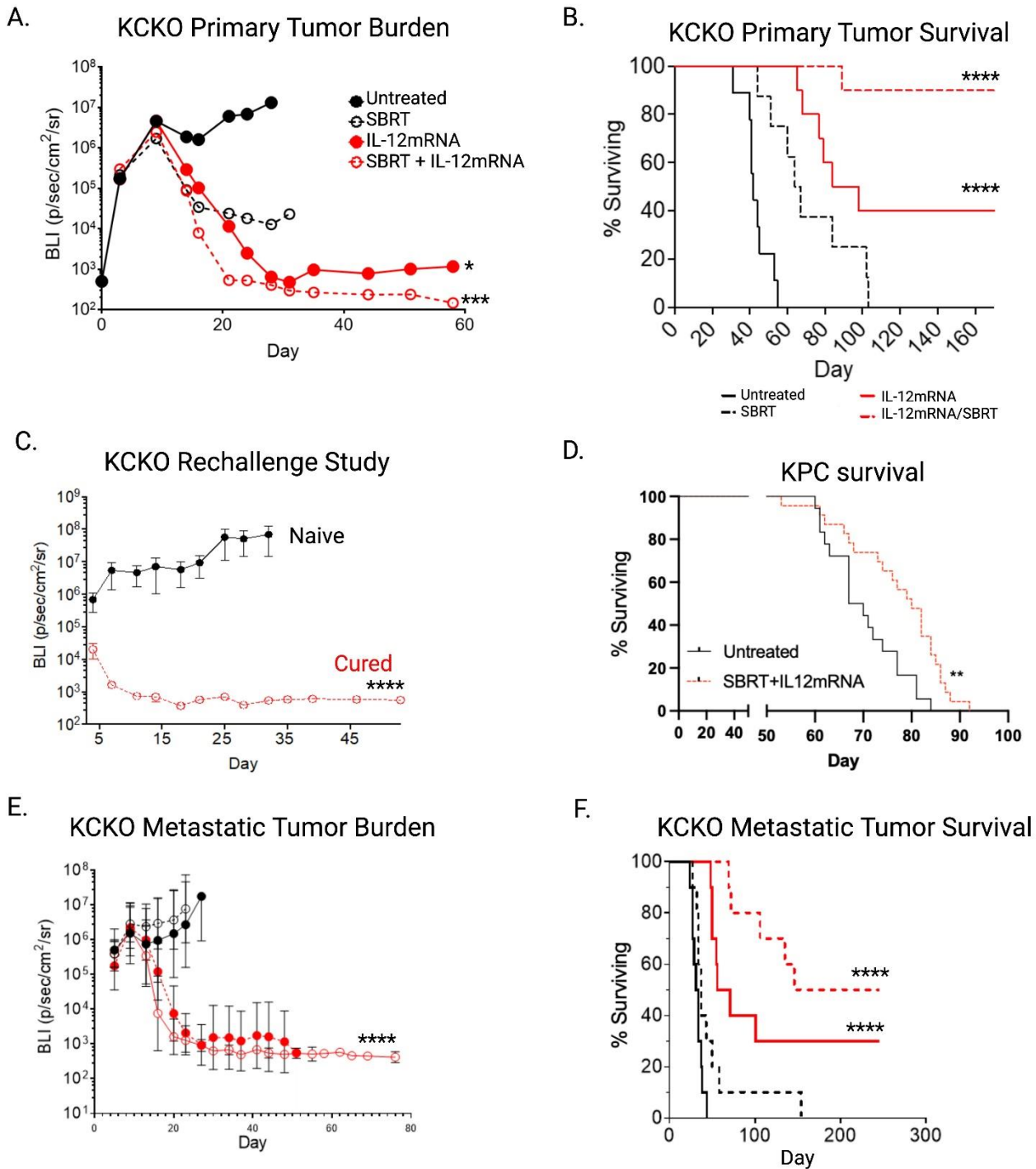


Figure S1. Combination treatment controls tumor burden and improves survival in multiple PDAC mouse models. (A) KCKO cells were injected orthotopically and treated with or without SBRT (6Gy/day over 4 consecutive days) followed by an intratumoral injection of IL-12mRNA or scr-mRNA 1 day after the final fraction of radiation. Tumor burden was assessed by BLI measurements. (B) Survival of KCKO model followed for >160 days. (C) Mice cured of KCKO tumors following SBRT and IL-12mRNA treatment for 150 days were rechallenged with a hemi-spleen injection of KCKO-Luc to induce hepatic metastases. Liver tumor burden was assessed by IVIS. Aged-matched naïve mice were used as controls. (D) KPC mice were assessed for tumor at 5 weeks of age and fiducial clips inserted accordingly. SBRT (6G/day over 4 consecutive days) followed by an intratumoral injection of IL-12mRNA or control scr-mRNA 1 day after the final fraction of radiation was administered and survival monitored. (E) KCKO primary tumors were implanted along with liver metastasis and primary tumors were treated with SBRT and IL-12mRNA. Tumor burden was measured by BLI. (F) Survival of metastatic KCKO model. n=10/group from 3 independent experiments in A & B; n=5 naïve and n=7 cured in C; n=18 for Untreated and n=23 for SBRT + IL-12mRNA in D. n=10 in E and F. *p<0.05; **p<0.01; ***p,0.001 ****p<0.0001. Error bars represent SEM in (C) and (E).

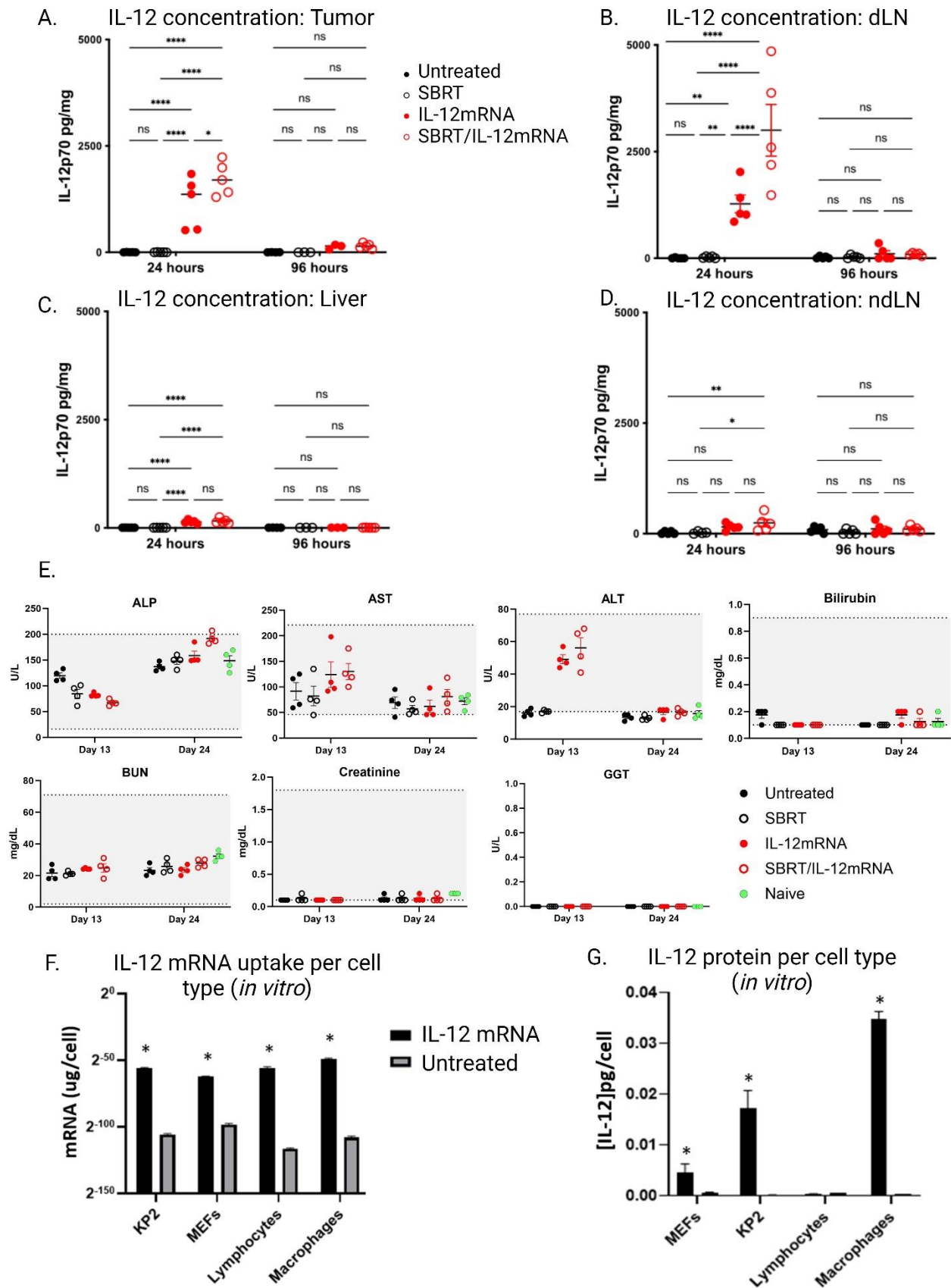


Figure S2. Assessment of IL-12 concentration following treatment. Mice were inoculated with KP2 tumor cells and treated as detailed in **Figure 1A**. 24 and 96 hours after intratumoral injection of IL-12mRNA or scr-mRNA, tissues were removed, homogenized, and assayed for IL-12p70 protein by Luminex. IL-12 concentration was determined following standardization to total protein (pg/mg) in **(A)** primary pancreatic tumors, **(B)** pancreatic tumor-draining lymph node, **(C)**

liver, and **(D)** non-draining (inguinal) lymph node. Y-axis is kept uniform to compare across tissues. **(E)** Mice were inoculated with KP2 tumors and treated as before. On days 13 and 24 post inoculation, serum was isolated from mice in each treatment group along with naïve, non-tumor bearing controls and assessed for biochemical analysis of liver (alkaline phosphatase: ALP, aspartate transaminase: AST, alanine transaminase: ALT, gamma-glutamyl transpeptidase: GGT, and bilirubin) and kidney function (blood urea nitrogen: BUN, and creatinine). Grey regions depict normal physiological levels for each respective marker. **(F)** Cultured cells consisting of KP2, mouse embryonic fibroblasts (MEFs), naïve CD4/CD8 lymphocytes, and peritoneal lavage macrophages were treated with IL-12mRNA or scr-mRNA *in vitro* for 24 hours and assayed for a unique sequence in IL-12mRNA by qPCR **(E)** or IL-12 protein by ELISA **(G)**. Values are standardized to number of total cells recovered at endpoint. n=5 mice/group in A-D; In E&F, each sample well was performed in triplicate and experiment repeated three times. Analyzed by one-way ANOVA followed by Tukey's test in A-D; student t-test in E&F comparing IL-12mRNA to scrRNA in each group. *p<0.05; **p<0.01; ****p<0.0001. Lines represent mean±SEM in **(A)** – **(E)** and error bars indicate SEM in **(F)** and **(G)**.

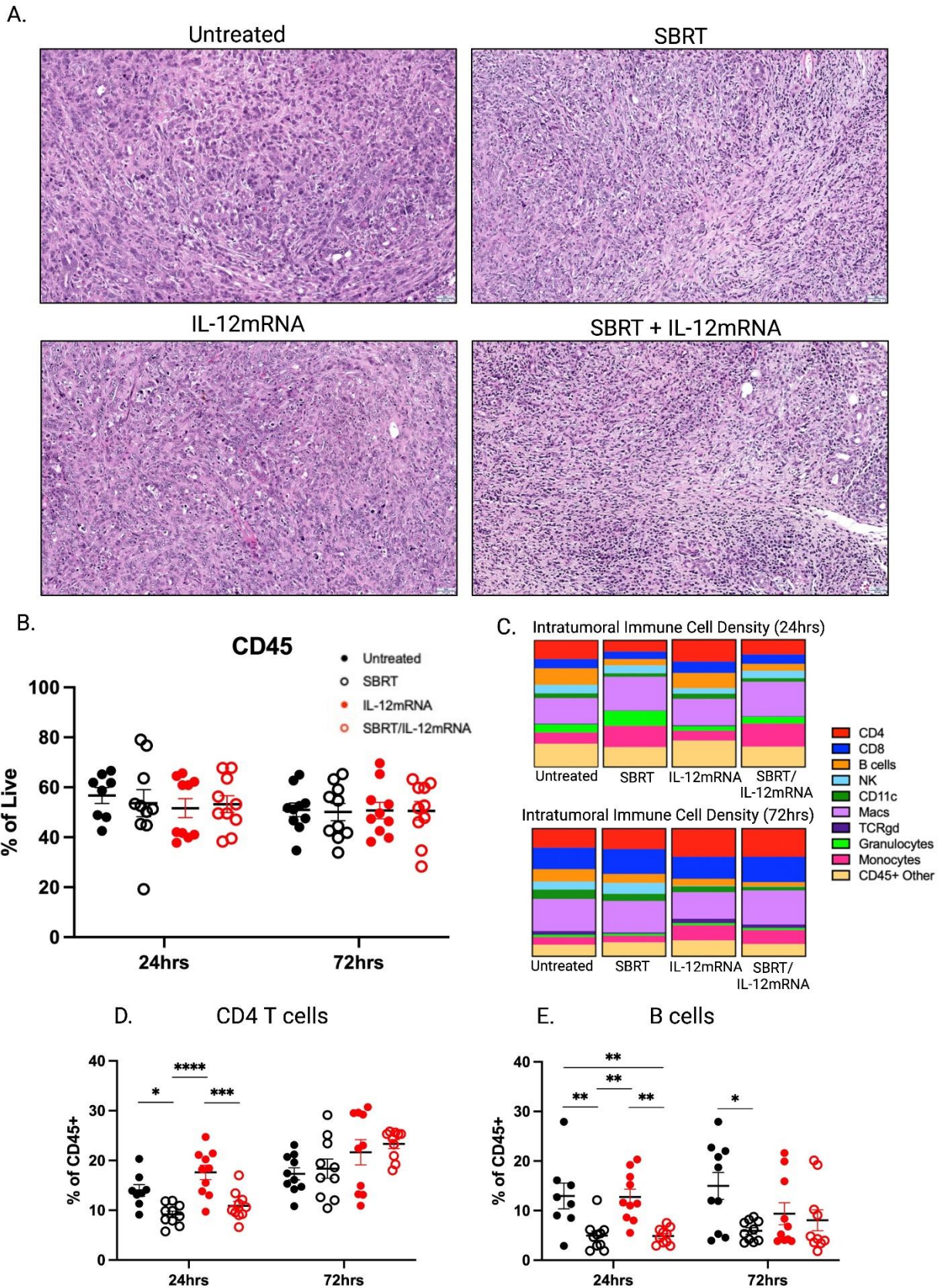


Figure S3. Effects of SBRT/IL-12mRNA on the tumor microenvironment. (A) Representative H&E images of tumors 72hrs post IL-12mRNA/scRNA injection (20X magnification). (B & C) Flow cytometry analysis of immune subsets across all treatments and time points. (D & E) Frequency of CD4 T cells and B cells 24hrs and 72hrs post IL-12mRNA/scr-mRNA injection for each treatment group. n=8-10 for B, D and E. Analyzed by one-way ANOVA followed by Tukey's test in C. *p<0.05; **p<0.01; ****p<0.0001. Scale bar represents 200um in A. Lines represent mean±SEM in (B), (D), and (E).

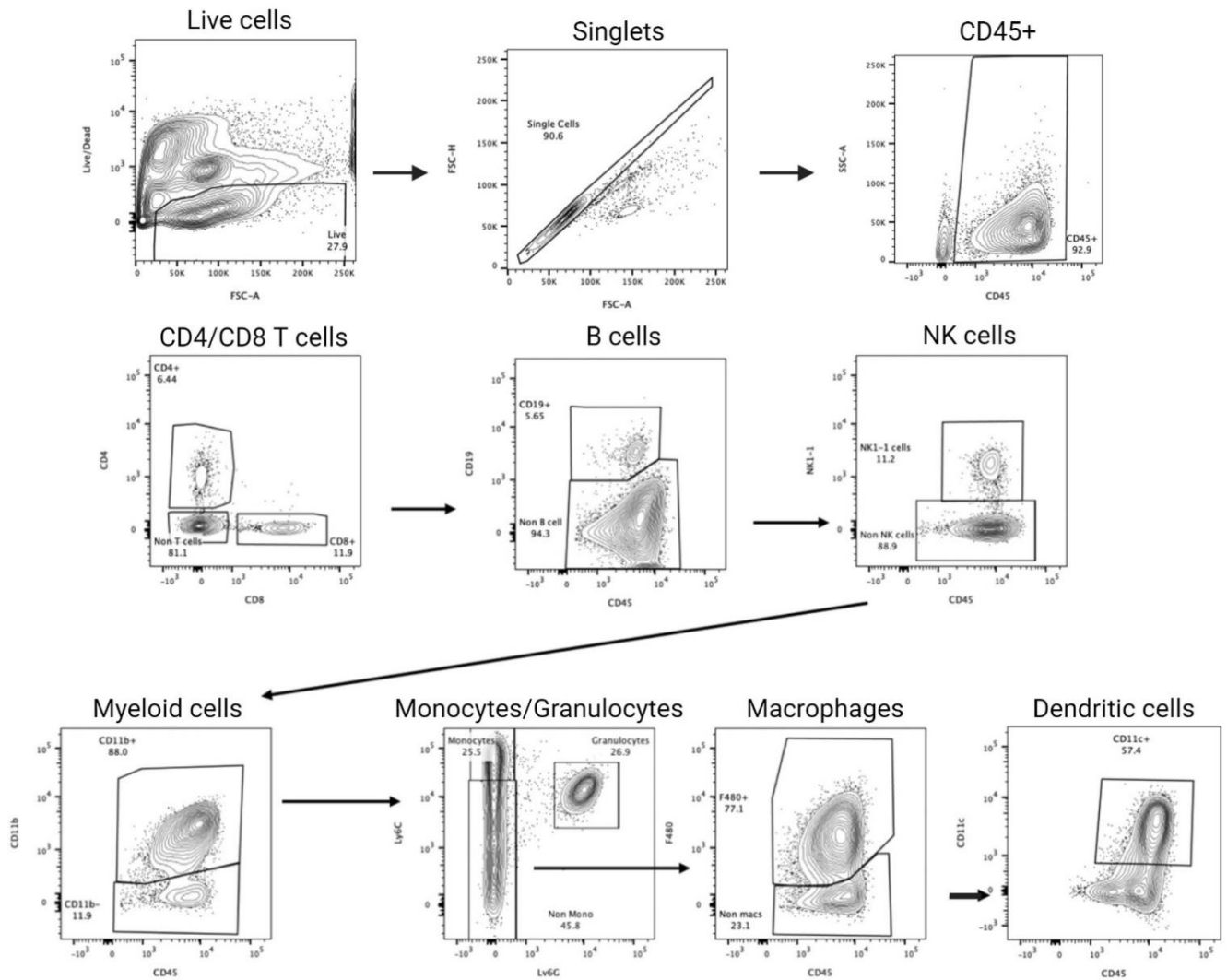


Figure S4: Gating strategy for determining immune subsets. Tumors were treated as described in **Figure 1A** and were harvested at 24 and 72 hours post IL-12 mRNA/scr-mRNA injection and stained for various markers to determine changes to immune subsets. Live cells (Ghost dye-) were gated against FSC-A and doublets were removed. CD45+ cells were gated and used to determine CD4+ and CD8+ T cells. Cells negative for CD4 and CD8 were used to gate B cells (CD19+), NK cells (NK1.1+) and myeloid cells (CD11b+). Myeloid cells were used to identify monocytes (Ly6C+), granulocytes (Ly6G+Ly6C+), macrophages (Ly6C-F480+) and dendritic cells (F480-CD11c+).

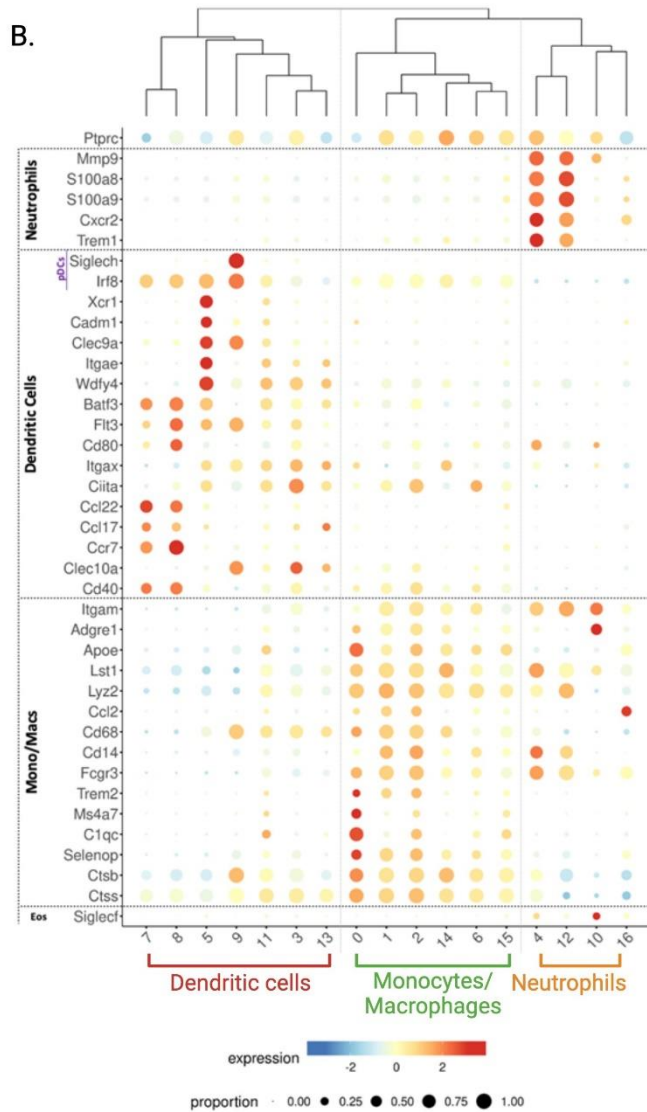
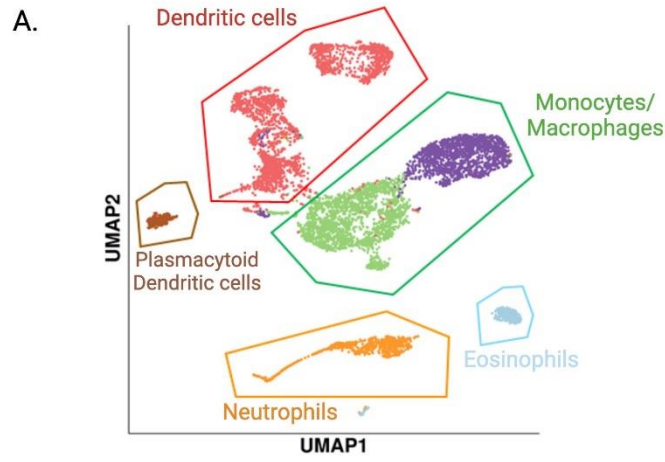


Figure S5. Identifying myeloid populations with scRNA-seq. (A) Combined UMAP of all myeloid cells used to identify populations of dendritic cells, monocytes/macrophages, neutrophils and eosinophils based on canonical markers. (B) Dot plots of canonical markers highlighting the different populations of myeloid cells.

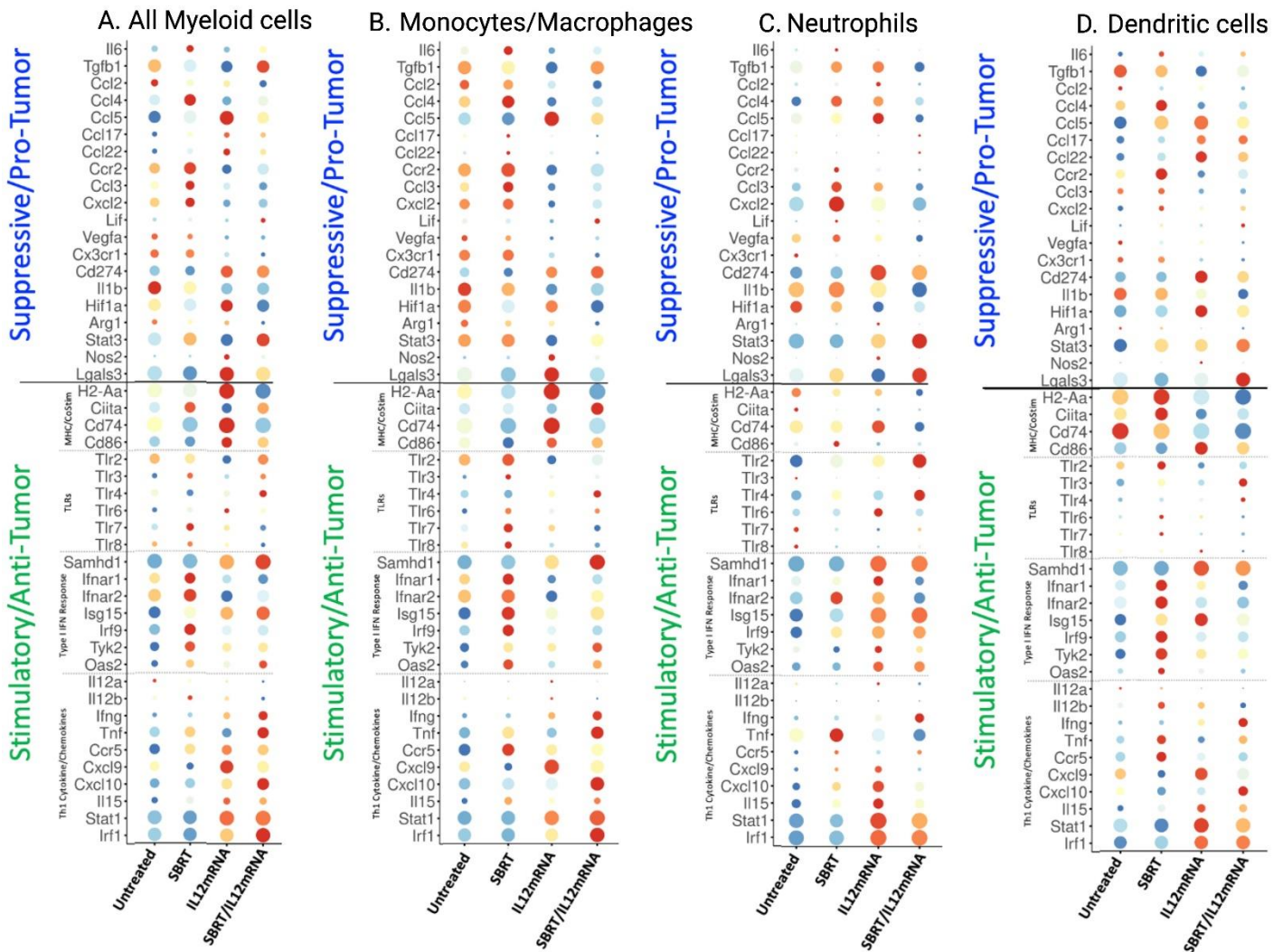


Figure S6. Expression of immunostimulatory and immunosuppressive genes in myeloid populations following treatment. Canonical immunostimulatory and immunosuppressive gene expression in (A) All Myeloid cells, (B) Monocytes and Macrophages, (C) Neutrophils and (D) Dendritic cells following treatment.

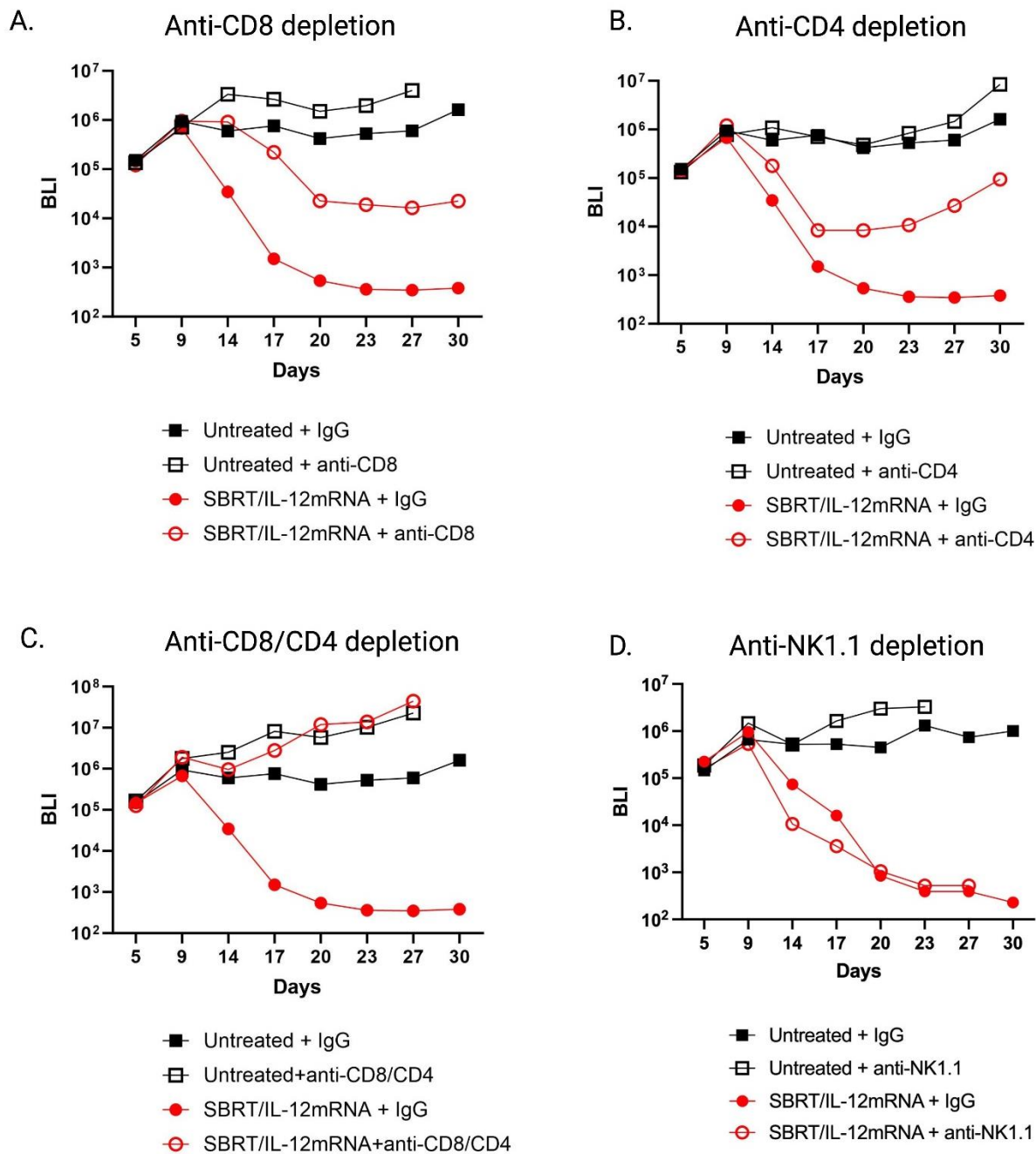


Figure S7. BLI growth curves following antibody depletion of effector cell populations during and after SBRT/IL-12mRNA treatment. (A) CD8 T cell depletion with isotype control for untreated and SBRT/IL-12mRNA treated mice. (B) CD4 T cell depletion with isotype control for untreated and SBRT/IL-12mRNA treated mice. (C) CD4 and CD8 T cell depletion with isotype control for untreated and SBRT/IL-12mRNA treated mice. (D) NK cell depletion with isotype control for untreated and SBRT/IL-12mRNA treated mice. In all cases, depletions began at Day 5 post tumor implantation (1 day prior to the first fraction of SBRT) and continued every 3 Days for a total of 7 doses. n=10 for each group.

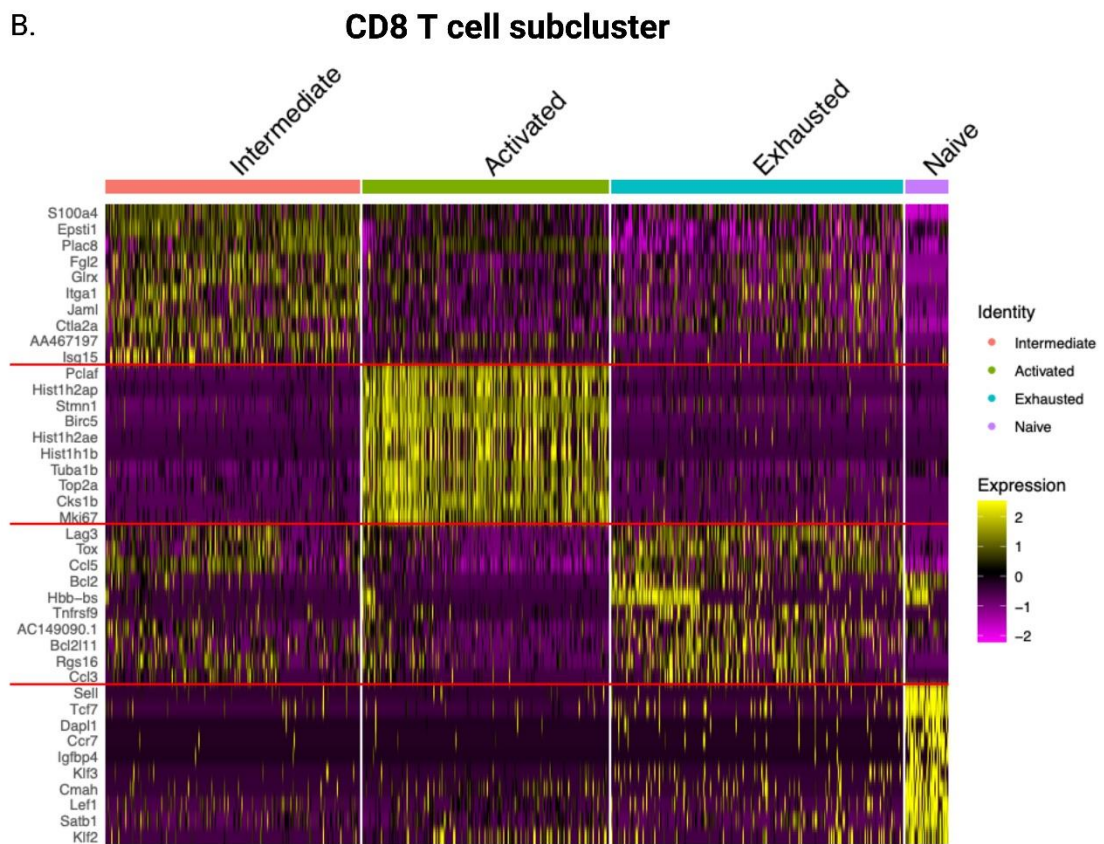
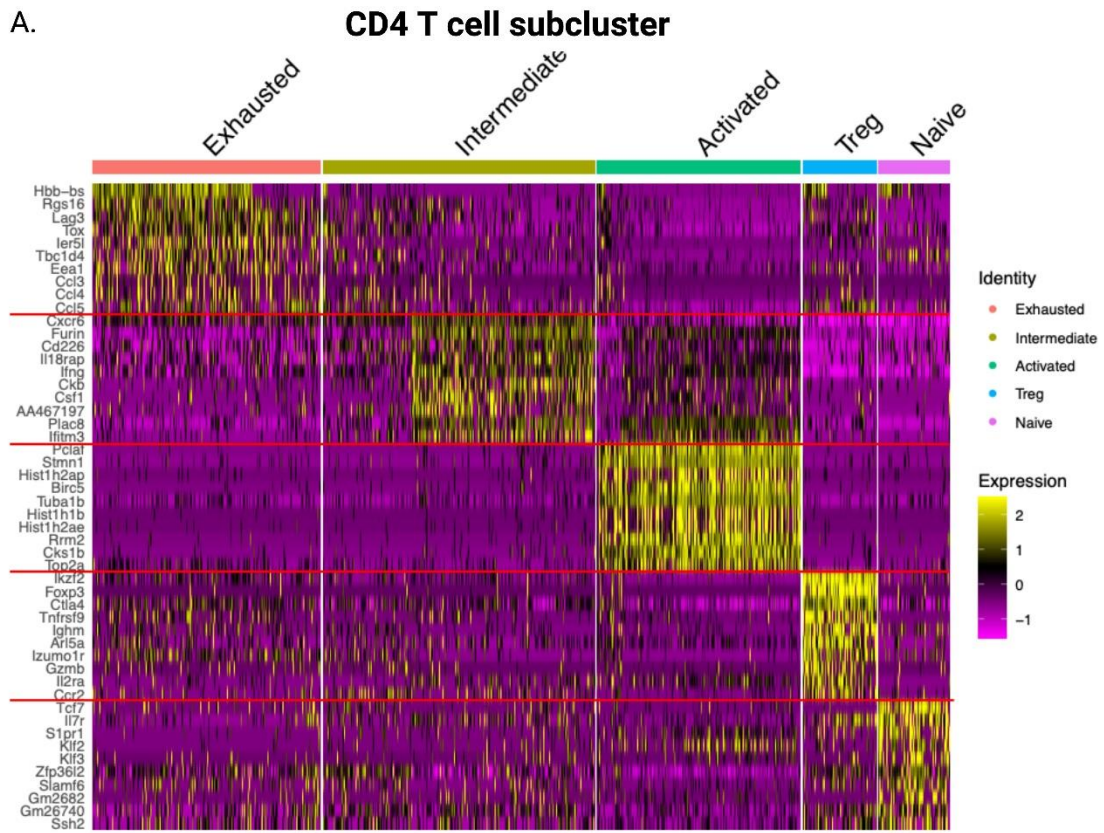


Figure S8. Differentially expressed genes for each subcluster of CD4 and CD8 T cells. Top 10 differentially expressed genes for each subcluster of CD4 (A) and CD8 (B) T cells are presented in heat maps.

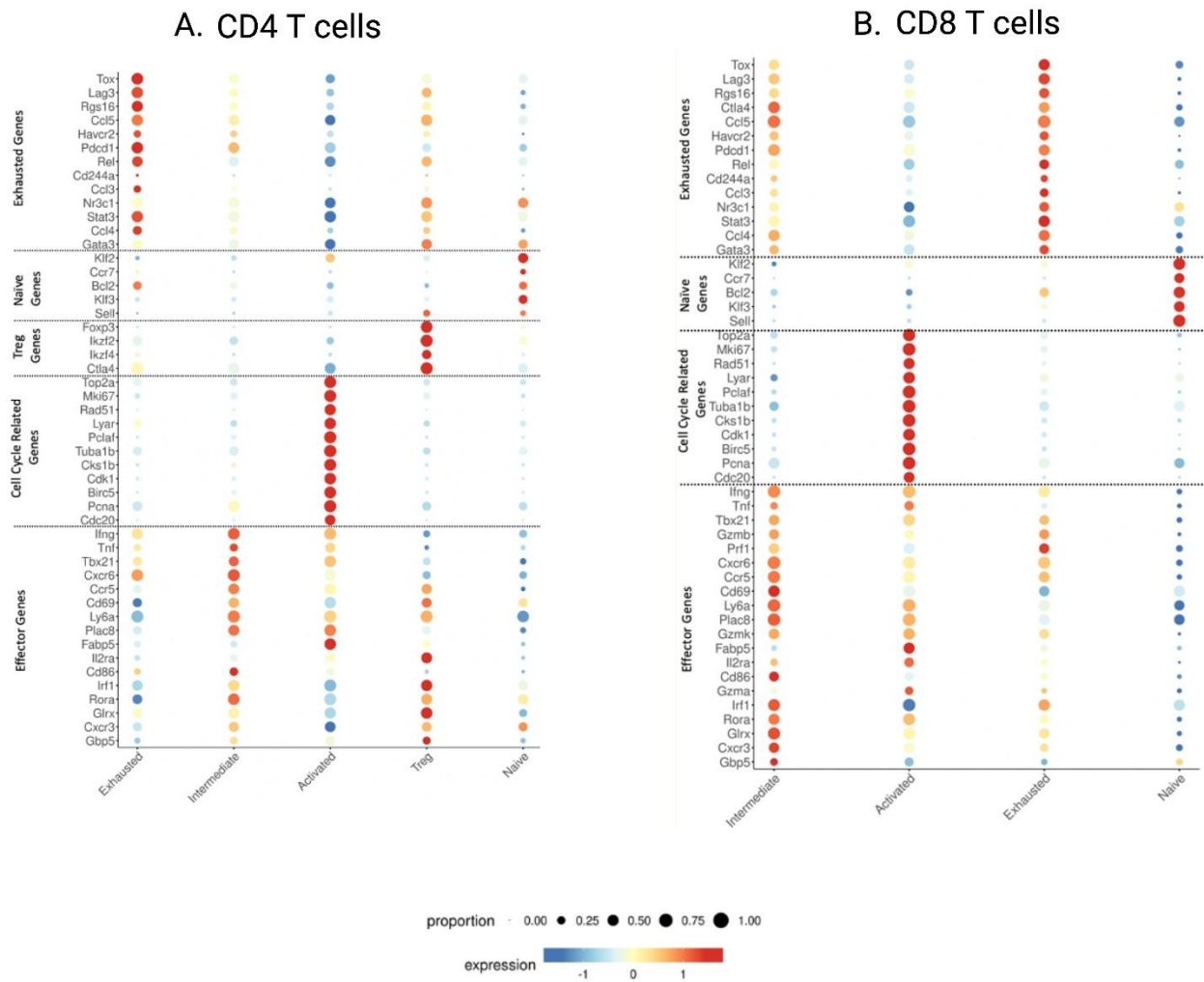
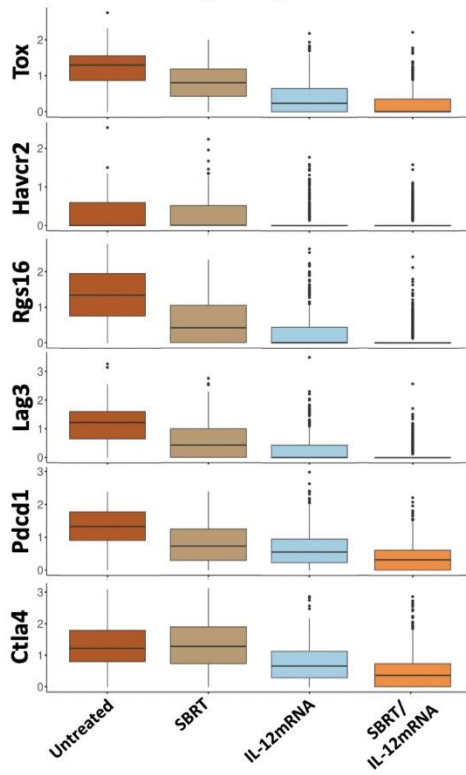
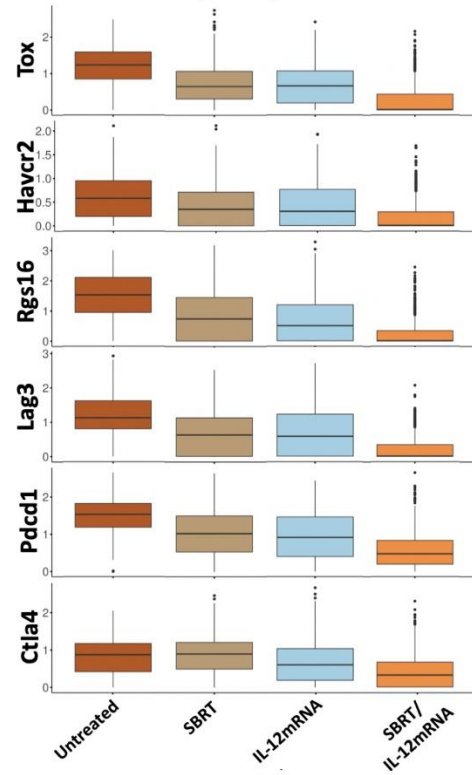


Figure S9. Classifying T cell subsets based on hallmark genes. Dot plots highlight expression levels of hallmark genes for a given proportion of cells associated with each subcluster of CD4 (A) and CD8 (B) T cells.

A. Activated/Cycling CD4 T cells



B. Activated/Cycling CD8 T cells



C.

CD8 T cells

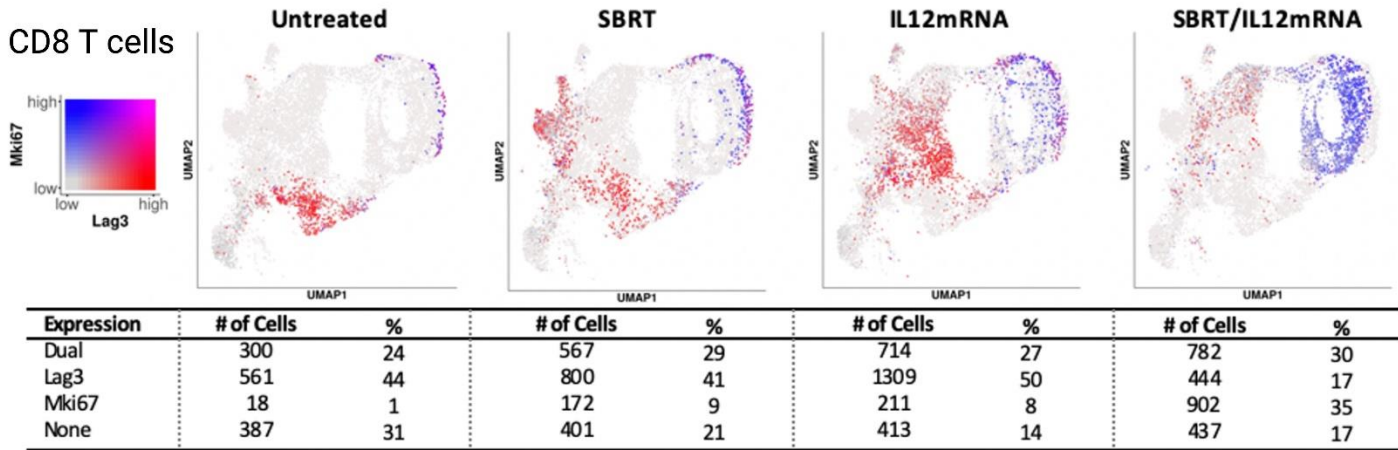


Figure S10. Expression of key genes in CD4 and CD8 T cells post treatment. (A & B) Boxplot depicting exhaustion marker expression in activated/cycling CD4 and CD8 T cells following treatment. **(C)** A marked reduction in exhaustion marker Lag3 is accompanied by an upregulation of proliferative marker Mki67 after SBRT/IL-12mRNA treatment.

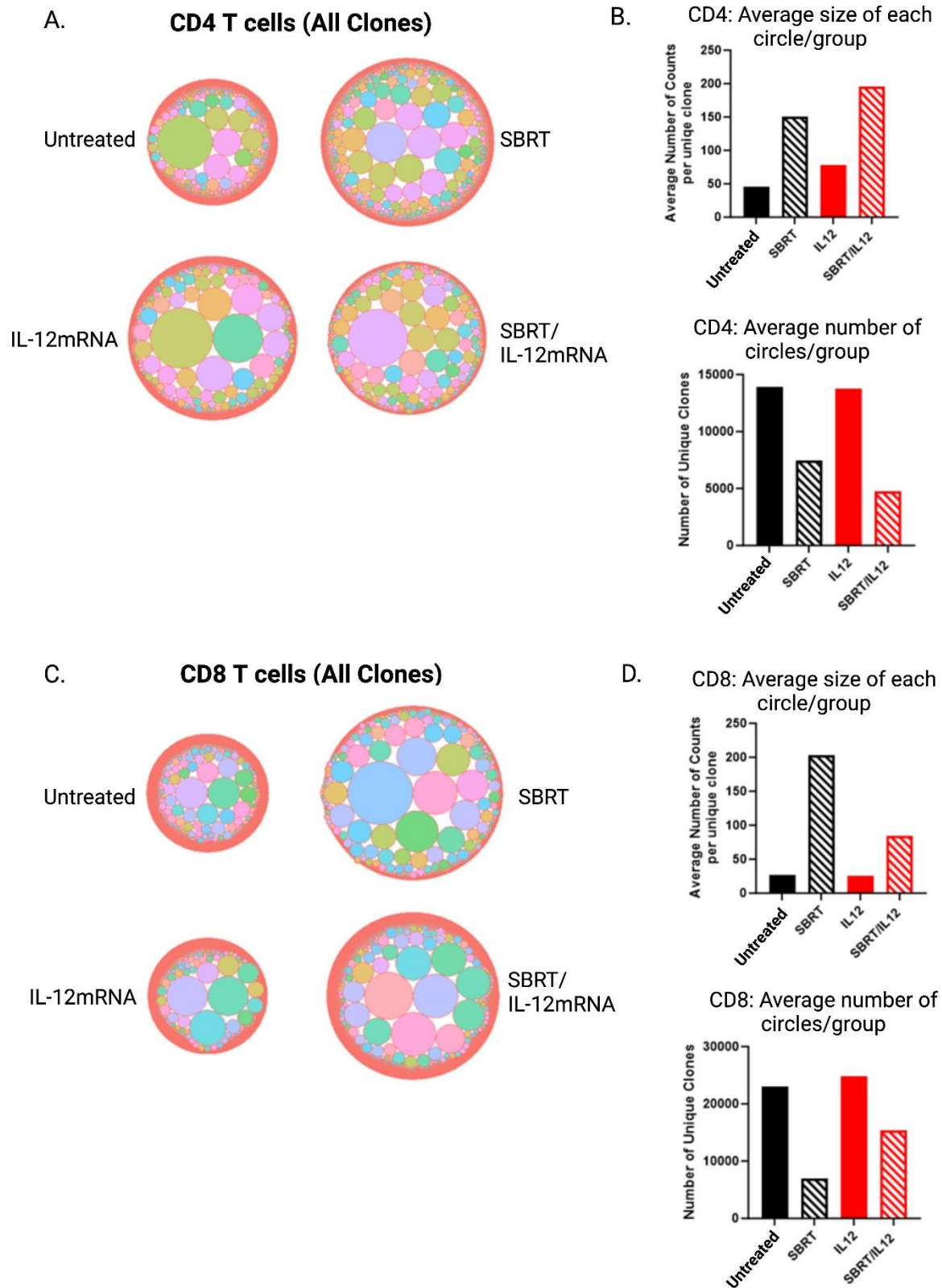
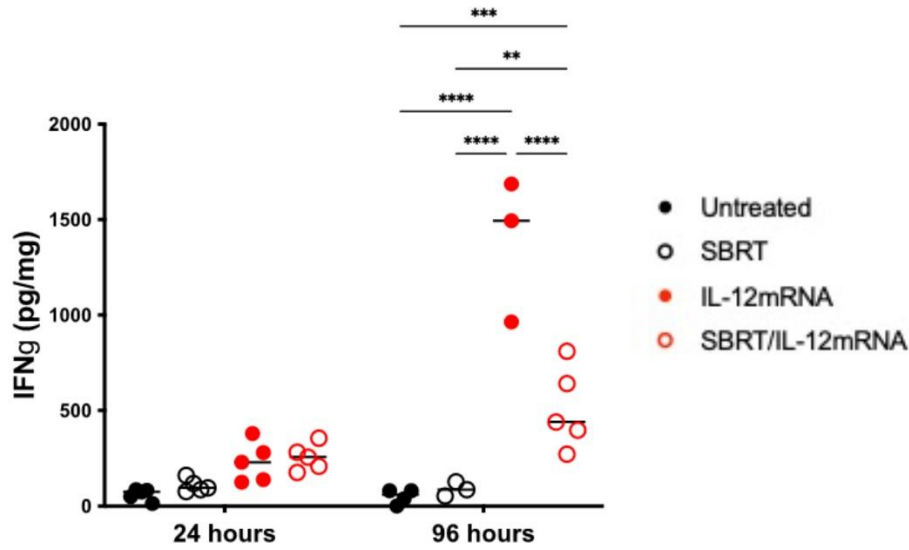


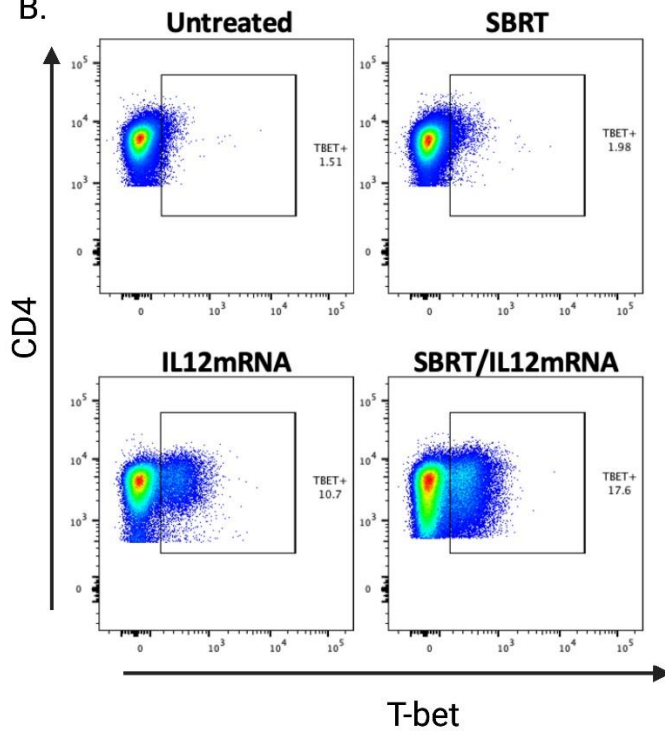
Figure S11. Downsampled population of CD4 and CD8 T cell clonotypes. Bubbleplots and accompanied bar charts depicting the downsampled size of T cell receptor clones and their relative abundance for CD4 T cells (**A & B**) and CD8 T cells (**C & D**).

A.

IFN γ concentration in pancreatic dLN



B.



C.

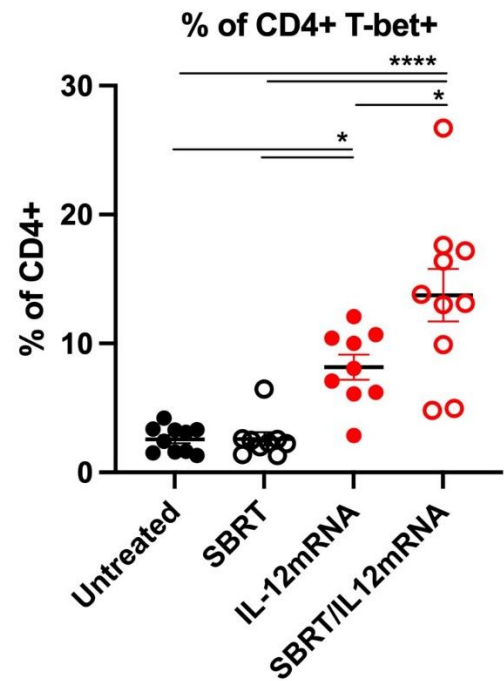


Figure S12. Quantifying IFN γ and T-bet expression in pancreatic draining lymph node following treatment. (A) IFN γ is significantly increased in the pancreatic draining lymph node 96 hours post IL-12mRNA/scr-mRNA injection. **(B)** Representative flow plots for T-bet staining of CD4 T cells. **(C)** Significant increases of T-bet+ CD4 T cells in the draining lymph node were determined at 72hrs post IL-12mRNA/scr-mRNA injection. Both A and C were analyzed by one-way ANOVA and Tukey's test. Significance is compared against the untreated and within treatments. n=5 for (A); n=9-10 for (B). *p<0.05; **p<0.01; ****p<0.0001. Lines represent mean \pm SEM in (C).

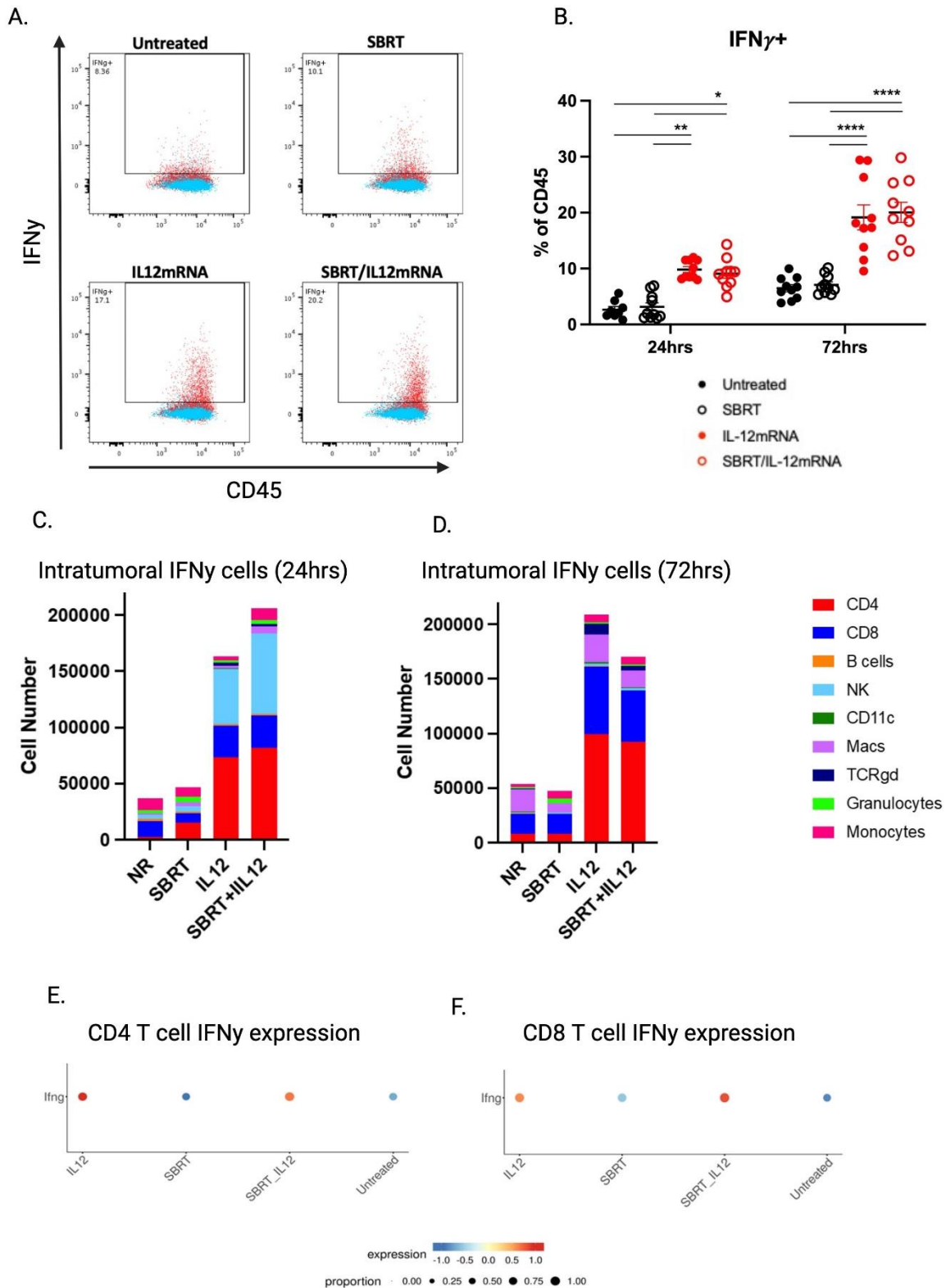


Figure S13. Expression of IFN γ in the tumor microenvironment following treatment. (A) Representative flow plots for IFN γ staining of CD45 $^{+}$ cells from the tumor microenvironment. Blue events indicate FMO control, red events correspond to IFN γ staining. (B) Tumor levels of IFN γ^{+} CD45 $^{+}$ cells 24hrs and 72hrs post IL-12mRNA/scr-mRNA injection. (C & D) Relative numbers of IFN γ^{+} intratumoral immune cells 24hrs and 72hrs post IL-12mRNA/scr-mRNA injection. (E & F) Gene expression of IFN γ^{+} by CD4 and CD8 T cells is mediated by IL-12mRNA. B was analyzed by one-way ANOVA followed by Tukey's test. * $p < 0.05$; ** $p < 0.01$; **** $p < 0.0001$. Lines represent mean \pm SEM in (B).